

Facile Synthesis and Electrical Conductivity of Carbon Nanotube Reinforced Nanosilver Composite

Hemant Pal^{a,d}, Vimal Sharma^a, Rajesh Kumar^b, and Nagesh Thakur^c

^a Department of Physics, National Institute of Technology, Hamirpur (H.P.) 177005 India

^b Department of Physics, Jaypee University of Information and Technology, Solan, (H.P.), 173212 India

^c Department of Physics, Himachal Pradesh University, Shimla (H.P.) 171005, India

^d Department of Physics, Govt. College Chowari, Chamba (H.P.), 176310, India

Reprint requests to H.P.; E-mail: hemantpal76@gmail.com

Z. Naturforsch. **67a**, 679–684 (2012) / DOI: 10.5560/ZNA.2012-0072

Received June 5, 2012 / revised July 20, 2012 / published online October 17, 2012

Metal matrix nanocomposites reinforced with carbon nanotubes (CNTs) have become popular in industrial applications. Due to their excellent thermophysical and mechanical properties, CNTs are considered as attractive filler for the improvement in properties of metals. In the present work, we have synthesized noncovalently functionalized CNT reinforced nanosilver composites by using a modified molecular level mixing method. The structure and morphology of nanocomposites are characterized by X-ray diffraction, scanning electron microscopy, transmission electron microscopy, and energy dispersive spectroscopy. The electrical conductivity of silver-CNT nanocomposites measured by the four-point probe method is found to be more than that of the pure nanosilver. The significant improvement in electrical conductivity of Ag/CNT nanocomposites stems from homogenous and embedded distribution of CNTs in a silver matrix with intact structure resulting from noncovalent functionalization. The low temperature sintering also enhances the electrical conductivity of Ag/CNT nanocomposites.

Key words: Ag/CNT; Nanocomposite; Molecular Level Mixing; Electrical Conductivity; Noncovalent Functionalization.

1. Introduction

A nanocomposite is a system comprising of two or more materials in which at least one phase is in the nanometer range [1]. These materials have emerged as suitable alternatives to overcome the limitations of conventional micro composites [2]. The carbon nanotubes (CNTs) are a promising raw material for industrial applications due to their outstanding properties [3]. Their application in conductive high strength composites [4] and interconnects [5] have received worldwide attention and interest. Owing to the excellent current carrying density, high electrical conductivity [6], and high aspect ratio, the CNTs have been used as reinforcement in metals to enhance the electrical properties [7]. A slight change in electrical conductivity has been observed in Cu/CNT [8–10] and Al/CNT composites [11], synthesized by conventional methods using covalently functionalized CNTs.

Silver has the highest electrical conductivity and CNTs have high mechanical strength, high thermal and electrical conductivities with a low coefficient of thermal expansion. Therefore, the integration of CNTs with silver is expected to produce nanocomposites with advantage of both. The silver matrix composites (Ag/CNT) have many electrical applications such as electrode materials [12], optical limiter, printed circuit boards in electronics [13], catalyst [14], electromagnetic interference (EMI) shielding, transparent conductive film, and in nanoelectronics [15]. Feng et al. [16] have reported an improvement in hardness with slight decrease in electrical conductivity of the Ag/CNT nanocomposite at high CNT volume per cent. The decrease in electrical conductivity is proposed due to creation of defects, shortening and agglomeration of CNTs in the silver matrix. However, it is not an easy task to get a homogenous distribution of CNTs in the metal matrix. The synthesis

method and functionalization of CNTs for their dispersion in the metal matrix play an important role. To overcome the problem of agglomeration of CNTs and to enhance interfacial bonding, Cha et al. [17] have proposed a new method for nanocomposite fabrication named as molecular level mixing. The results of this method show well embedded and homogeneously distributed CNTs in nanocomposites as compared to the conventional synthesis techniques. In the reported literature, only covalently functionalized CNTs have been used, though the covalent functionalization creates voids, defects and even reduces the aspect ratio which decreases the ballistic electrical conductivity due to increase in collision and scattering of the electrons at the defects [18]. Keeping in view the merits and demerits of available studies, the present work aims at the effect of noncovalently functionalized CNTs on the electrical conductivity of nanosilver matrix nanocomposite using the modified molecular level mixing method.

2. Experimental

In the synthesis of Ag/CNT, nanocomposite multiwall (MW) CNTs (Nanoshell, purity 90–98 vol %) of diameter 4–12 nm and length 15–30 μm have been used. Three samples of Ag/CNT nanocomposites with 0, 6, and 12 vol% CNTs have been prepared by a modified molecular level mixing method using surfactant assisted noncovalently functionalized CNTs. The MW-CNTs powder of said percentages was dispersed in ethanol using an ultrasonic probe sonicator at high frequency. Then 0.2 gm of sodium lauryl sulphate (Fisher Scientific, purity 99%) was added into the solution and sonicated for 2 hours to get a homogenous dispersion of CNTs. Silver nitrate (Fisher Scientific, purity 99.8%) was added to the CNT suspension and the solution was slowly stirred continuously for 12 hours covering with black sheet to avoid the direct light. 2 ml hydrazine hydrate (Merck, purity 99%–100%) was added to this solution which caused a change in the color of the solution from black to light brown confirming the synthesis of silver nanopowder. The so obtained Ag/CNT was separated from the solution by centrifugation for 5–10 minutes at the speed of 5000 rpm. This nanocomposite powder was heated up to 50 $^{\circ}\text{C}$ to evaporate the solvent. The obtained powder was further washed repeatedly with deionized water to remove the surfactant. Finally, Ag/

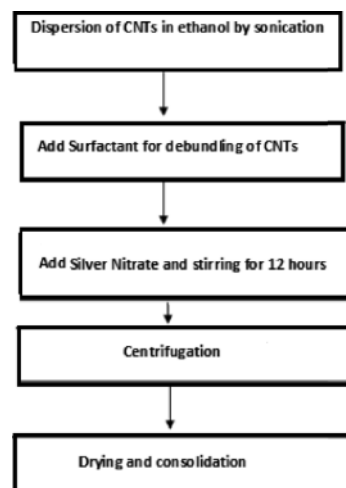


Fig. 1. Schematic of Fabrication process.

CNT powdered nanocomposite was obtained after drying the sample at 40–50 $^{\circ}\text{C}$ on a hot plate. This nanopowder was further consolidated into cylindrical pellets of diameter 13 mm and thickness of nearly 1 mm by a simple graphite moulding press by applying a pressure of 1.5 tones. The pellets were used for studying the V – I characteristic and the sintering behaviour. The microstructure of Ag/CNT nanocomposite powder was investigated by X-ray diffraction (XRD), scanning electron microscopy (SEM), transmission electron microscopy (TEM), and energy dispersive spectroscopy (EDS). The electrical conductivity measurements were performed using a four-point probe electrometer (Kiethly2400 source meter and nano voltmeter). The schematic of the fabrication process is shown in Figure 1.

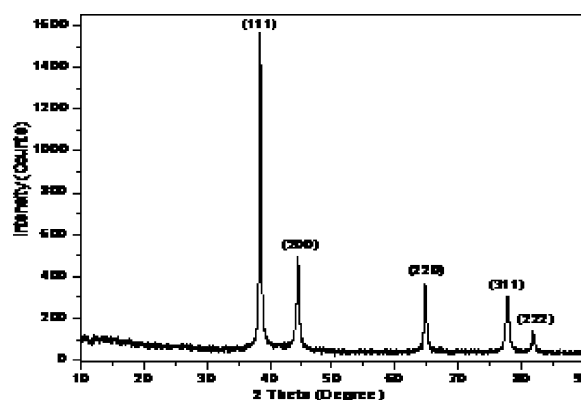


Fig. 2. XRD of Ag/MW-CNT nanocomposite.

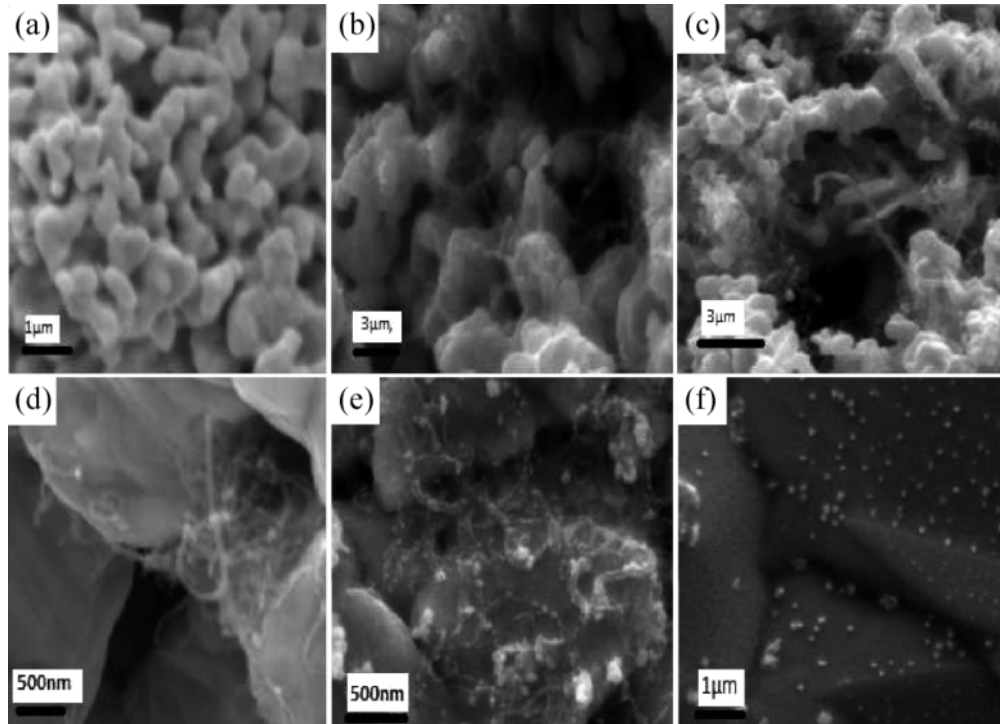


Fig. 3. SEM micrographs of Ag/MW-CNT nanocomposite. (a) Pure nanosilver (0 vol % CNTs) nanopowder; (b) and (c) Ag/CNT (6 vol %) nanocomposite powder showing uniformly distributed CNTs in the matrix; (d) agglomerates of CNTs in Ag/CNT (12 vol %) nanocomposites; (e)–(f) unsintered and sintered Ag/CNT (6 vol %) pellets highlighting uniform distribution of CNTs.

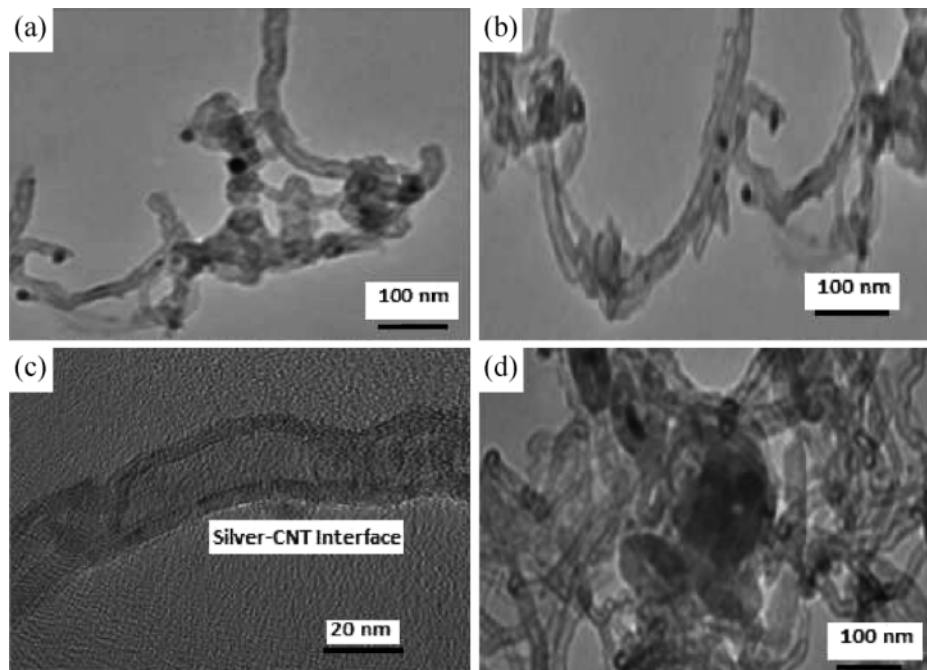


Fig. 4. TEM micrographs of Ag/MWCNT nanocomposite. (a) and (b) Ag/CNT (6 vol %) nanocomposite showing uniform distribution of CNTs in the matrix; (c) Ag/CNT (6 vol %) nanocomposite showing silver-CNT interface; (d) agglomerates of CNTs in Ag/CNT (12 vol %) nanocomposites.

3. Experimental Results

3.1. Morphology and Structural Characterizations

The XRD patterns of Ag/CNT (6 vol %) nanopowder shown in Figure 2 indicate the crystalline nature of the sample with peaks corresponding to the face centered cubic (FCC) structure of the silver nanoparticles. The major diffraction peaks at 38.9° , 45.1° , 65.1° , and 78.2° corresponds to (111), (200), (220), and (311) reflections of FCC phase of silver.

By calculating the line broadening in diffraction patterns and applying the Debye–Scherer formula, a crystallite size of 58 nm has been obtained. There is no specific well defined peak for multiwalled CNT due to their small volume percentage and uniform distribution in the silver matrix; however a slight hump in the curve from base line between 2θ values of $15^\circ - 25^\circ$ indicates the presence of CNTs in the sample.

The SEM micrographs of Ag/CNT nanocomposite with different CNT volume per cent are shown in Figure 3a–f. The Ag/CNT nanopowder with 6 vol % CNTs shows homogeneously dispersed, intact, and embedded CNTs in the silver matrix. On the other hand, the Ag/CNT with 12 vol % CNTs shows agglomeration of CNTs. Figure 3e and f highlight the SEM micrographs of unsintered and sintered pellets of Ag/CNT nanocomposite, respectively, with 6 vol % CNTs. These micrographs confirm the uniform distribution of CNTs in the silver matrix.

The TEM micrographs in Figure 4a–c show individually dispersed CNTs with their intact structure in Ag/CNT (6 vol %), and Figure 4d shows the presence

of CNT aggregates in Ag/CNT (12 vol %) nanocomposite.

In order to determine the elemental composition of Ag/CNT nanocomposite, the elemental analysis was carried out employing EDS. The weight percentage of the CNTs in the Ag/CNT nanocomposite as shown in Figure 5 confirm the presence of approximate 12 vol % CNTs in the composite.

3.2. Electrical Measurements

The electrical conductivity was measured using a standard four-point probe method. All conductivity measurements were performed at room temperature. The CNT weight percentage, density, and electrical conductivity of the samples are shown in the Table 1.

For each sample, the conductivity data represent the average value of 10 consecutive measurements on three set of samples. It is clear from Figure 6 that the Ag/CNT nanocomposites with 0, 6, and 12 vol % CNTs loadings follow Ohm's law and have characteristic lines with different slopes showing different conductivities. It has been found that the electrical conductivity of the Ag/CNT nanocomposites is higher

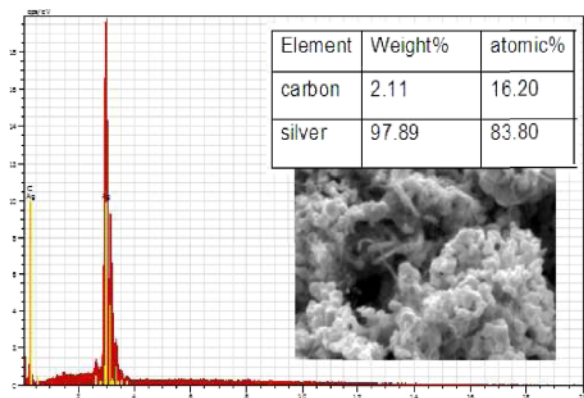


Fig. 5 (colour online). EDS analysis of Ag/MW-CNT nanocomposite.

Table 1. Density and electrical conductivity of Ag/MW-CNT nanocomposites.

Specimen	Conductivity [s/m]	CNT [mg]	Silver nitrate	CNT vol %	Density [mg/cm ³]
Ag	$0.4 \cdot 10^7$	0	3 gm	0	8.62
Ag/CNT	$0.9 \cdot 10^7$	11	3 gm	6	7.72
Ag/CNT	$0.7 \cdot 10^7$	22	3 gm	12	7.46

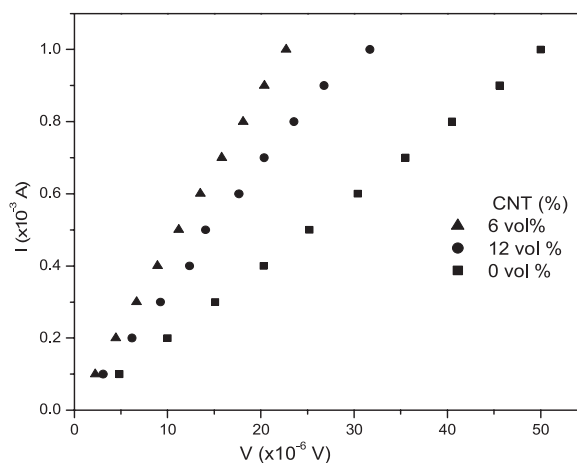


Fig. 6. $V-I$ Characteristics of Ag/MW-CNT nanocomposite.

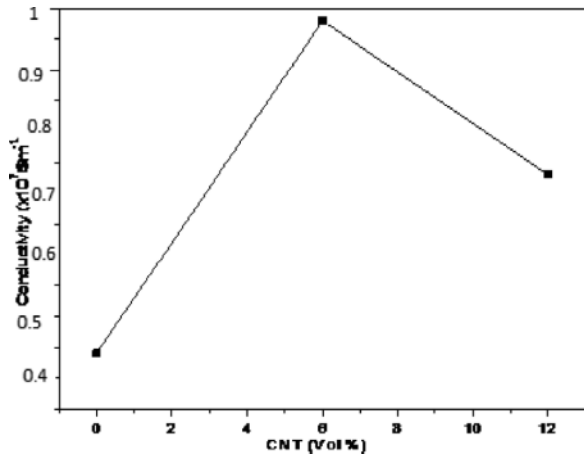


Fig. 7. Electrical conductivity of Ag/MW-CNT nanocomposite with MW-CNT volume percentage.

than that of the pure nanosilver (0 vol % CNTs) and increases to twice at 6 vol % of CNTs as shown in Figure 7. The numerical value of the electrical conductivity depends on the consolidation pressure and CNT volume percentage in the matrix.

3.3. Low Temperature Sintering of Ag/CNT Nanocomposites

The sintering and densification processes directly affect the electrical properties because during sintering, the particles bond together and the pores shrink. Due to the low melting point of silver nanoparticles, the low temperature sintering behaviour of Ag/CNT nanocomposite has been studied. Ag/CNT nanocomposite pellets were sintered in a muffle furnace at 100, 150, and 200 °C for 10 minutes in each step. The elec-

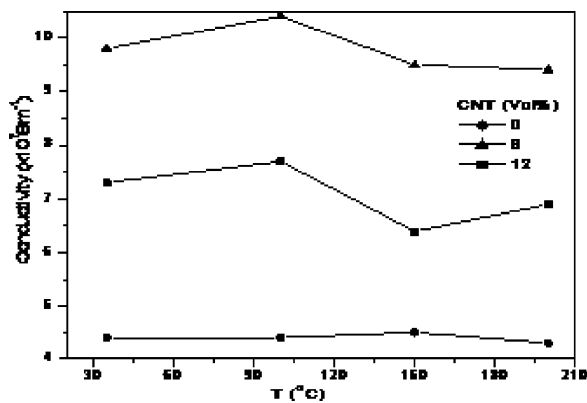


Fig. 8. Sintering of Ag/MW-CNT nanocomposite.

trical conductivity of these samples was measured as the average value of 10 consecutive measurements with rise of temperature. From Figure 8 it is clear that up to a sintering temperature range 100 °C, the electrical conductivity of pure silver pellet remains almost constant and increases slightly from 100 to 150 °C and then decrease beyond the 150 °C. While in CNT reinforced silver matrix nanocomposites (6 vol % and 12 vol %) the electrical conductivity increases within a temperature range of 35–100 °C and then decreases at 150 °C. This is due to the presence of more pores in the matrix which provide easy path for the expansion even at low temperature. Coalescence of the Ag nanoparticles during the sintering process increases the density [19] and hence the conductivity of the nanocomposites. At higher temperature, the grain size starts increasing which further reduces the electrical conductivity.

4. Discussion

Due to high current carrying capacity (10^9 A/cm^2) and low resistivity of individual multiwall CNTs [20], these can be used as reinforcement for improvement of electrical conductivity in metal matrix nanocomposites. But the reported results show a decrease in electrical conductivity when covalently functionalized CNTs are reinforced in a metal matrix [16]. Chemical covalent functionalization of CNT is a double edge sword which increases its dispersion in the solution as well as enhances the interfacial bonding of CNTs with the matrix. However at the same time, it also creates many defects and voids in the structure of CNT which may increase the scattering of the electrons, and hence the electrical conductivity decreases [21]. The surfactant aided noncovalent functionalization based on the physical adsorption of the surfactants is widely adopted to obtain homogenous CNT suspension, taking the advantage of leaving the electronic structure intact [22]. It creates the bonding between metal matrix and CNTs by $\pi - \pi$ stacking without disturbing the normal structure [23].

The electrical conductivity of Ag/CNT nanocomposites for all CNT volume per cent is more than that of the pure nanosilver (0 vol % CNTs). Specifically, the value of the electrical conductivity for 6 vol % CNT composite is maximum to the extent of nearly twice the value for pure nanosilver (0 vol % CNTs). This sharp increase in electrical conductivity for 6 vol % of

CNTs nanocomposite has been assigned to a homogeneous distribution of CNTs in the silver matrix as evidenced by SEM and TEM micrographs. Agglomeration of CNTs occurs with increase in CNT volume per cent in the silver matrix which results in the decrease in electrical conductivity. Thus, a significant improvement in electrical conductivity of Ag/CNT nanocomposites has been shown (Fig. 9) to stem from the homogenous and embedded distribution of CNTs

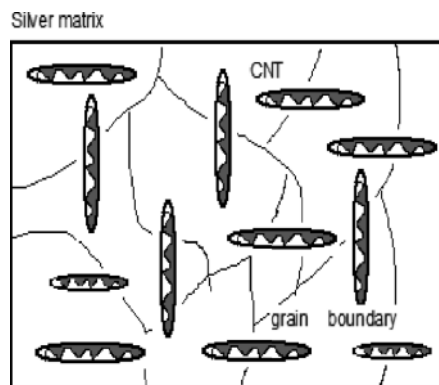


Fig. 9. Schematic of Ag/MW-CNT nanocomposite.

in nanosilver matrix with an intact structure resulting from noncovalent functionalization.

5. Conclusions

The Ag/CNT nanocomposites fabricated by employing noncovalently functionalized CNTs through a modified molecular level mixing method. The study shows an intact, embedded, and homogenous distribution of the CNTs in the silver matrix connecting the grain boundaries. Consolidated and low temperature sintered Ag/CNT nanocomposites have enhanced the electrical conductivity. The electrical conductivity of Ag/CNT nanocomposite at 6 vol % CNT has been enhanced more than twice as compared to pure nanosilver (0 vol % CNT). These interesting preliminary results are under further optimization to validate in more comprehensive manners so that these may be put into use in future applications.

Acknowledgement

The authors thankfully acknowledge the financial support from Department of Science and Technology [Project-SR/FTP/PS-054/2011(G)], India.

- [1] H. Dai, *Acc. Chem. Res.* **35**, 1035 (2002).
- [2] P. Ngoc and P. H. Khoi, *J. Phys. Conference Series* **187**, 012002, (2009).
- [3] M. Endo, T. Hayashi, Y. A. Kim, M. Terrones, and M. S. Dresselhaus, *Phil. Trans. R. Soc. Lond. A* **362**, 2223 (2004).
- [4] R. H. Baughman, A. A. Zakhidov, and W. A. de Heer, *www.sciencemag.org SCI*, 297, (2002).
- [5] M. Endo, T. Hayashi, Y. A. Kim, and H. Muramatsu, *AAPPS Bulletin* **18**, 1 (2008).
- [6] S. R. Bakshi, D. Lahiri, A. Agarwal, *Int. Mater. Rev.* **55**, 41 (2010).
- [7] T. W. Ebbesen, H. J. Lezee, H. Hiura, J. W. Bennett, H. F. Ghaemie, and Thio, *Nature* **382**, 54 (1996).
- [8] S. Baik, B. Lim, S. Ryu, D. Choi, B. Kim, S. Oh, B. Sung, J. H. Choi, and C. J. Kim, *Solid State Phenomena* **120**, 285 (2007).
- [9] B. K. Lim, C. B. Mo, D. H. Nam, and S. H. Hong, *J. Nanosci. Nanotech.* **10**, 78 (2010).
- [10] W. M. Daush, *Powder Metal Metal Ceramics* **47**, 9 (2008).
- [11] C. L. Xu, B. Q. Wei, R. Z. Ma, J. Liang, X. K. Ma, and D. H. Wu, *Carbon* **37**, 855 (1999).
- [12] J. Śleziona, J. Wiczorek, and M. Dyzia, *J. Achievements Mater. Manufacturing Eng.* **17**, 1 (2006).
- [13] W. Guchowski and Z. Rdzawski, *J. Achievements Mater. Manufacturing Eng.* **30**, 2 (2008).
- [14] K. C. Chin, A. Gohel, W. Z. Chen, H. I. Elim, W. Ji, Chong GL, C. H. Sow, and A. T. S. Wee, *Chem. Phys. Lett.* **409**, 85 (2005).
- [15] B. Xue, P. Chen, Q. Hong, J. Y. Lin, and K. L. Lin, *J. Mater. Chem.* **11**, 2378 (2001).
- [16] Y. Feng, H. L. Yuan, and M. Zhang, *Mater. Charact.* **55**, 211 (2005).
- [17] S. I. Cha, K. T. Kim, S. N. Arshad, C. B. Mo, and S. H. Hong, *Adv. Mater.* 1377, (2005).
- [18] T. Tasis, N. Tagmatarchis, V. Geogakilas, and M. Prato, *Chem. Eur. J.* **9**, 4000 (2003).
- [19] K. S. Moon, H. Dong, R. Maric, S. Pothukuchi, R. Hunt, Y. Li, and C. P. Wong, *J. Electronic Mater.* **34**, 2 (2005).
- [20] M. Torrens, *Int. Mater. Rev.* **49**, 325 (2004).
- [21] X. M. Sui, S. Giordani, M. Parto, and H. D. Wagner, *Appl. Phys. Lett.* **95**, 233113 (2009).
- [22] C. Y. Hua, Y. J. Xu, S. W. Duo, R. F. Zhang, and M. S. Li, *J. Chinese Chem. Soc.* **56**, 234 (2009).
- [23] L. Vaisman, Wagner, and G. Marom, *Adv. Colloid Interface Sci.* **37**, 128 (2006).